Vapor-liquid coexistence of fluids with attractive patches: An application of Wertheim's theory of association

Hongjun Liu,[1] Sanat K. Kumar,[1,a)] Francesco Sciortino,[2,b)] and Glenn T. Evans[3,c)]
[1]*Department of Chemical Engineering, Columbia University, New York 10027, USA*
[2]*Department of Physics and INFM-CNR-SOFT, University of Roma La Sapienza, 00185 Roma, Italy*
[3]*Department of Chemistry, Oregon State University Corvallis, Oregon 97331, USA*

(Received 19 September 2008; accepted 11 December 2008; published online 23 January 2009)

We compare simulations and theoretical predictions based on Wertheim's thermodynamic perturbation theory (TPT) for spheres that interact through an isotropic square well interaction coupled to patchy attractions. Following a proposal of Foffi and Sciortino [J. Phys. Chem. B **111**, 9702 (2007)], we show that, if we use the second virial coefficient as a scaling parameter, a generalized law of corresponding states holds not only for the critical point but also for the vapor-liquid coexistence curve of patchy hard sphere fluids with the same numbers of single-bonded patches. The predictions for patchy square well fluids from Wertheim's TPT are in good agreement with Monte Carlo simulation data, although no aspects of universality were found. Instead, we find a crossover from the behavior of isotropically short-ranged attractive fluids to that of patchy hard sphere fluids as the strength of patchy interaction increases. © *2009 American Institute of Physics*. [DOI: 10.1063/1.3063096]

I. INTRODUCTION

The idea of modeling proteins as spherical particles with anisotropic, as opposed to isotropic, short-ranged attractions has received considerable attention recently.[1–9] Although models equipped with isotropic pair potentials have been successful in predicting the thermodynamic and dynamical properties of many systems, intermolecular interactions between proteins are intrinsically directional. The highly directional attraction has many nonbiological precedents, e.g., in network forming systems[10–14] such as water,[15–19] silica, and for many associating fluids[20] (alcohols and amines). When patchy sites or domains are distributed on the particle surface, extended networks can result. Further, it has been shown that the number of patches (or the valence) is a key ingredient in controlling the phase diagram of patchy particles. Through adjusting the valence, low-density or "empty" liquids are accessible.[21] The patchy model is also related to the self-assembly of functionalized colloidal particles. There has been increasing interest in the synthesis of colloidal molecules,[22,23] which might be used as building blocks of specifically designed structures. One ambitious target is to assemble the particles with tetrahedral symmetry into a diamond structure.[24]

Wertheim's thermodynamic perturbation theory (TPT)[25–27] is a graph-theoretic approach that describes particles with short-ranged highly directional forces. The interaction spots can bond with at most one other spot on a nearby molecule. In the simplest form of TPT, the interaction spots are located randomly on the surface on the particle: Hence the geometry of the clusters formed via an application of TPT will not be correct. However, the resultant predicted single-bonded networks have been useful for studying the statics of polymer chains, as evidenced in comparisons of theory with simulation.[28]

The conical reactive spot is a good model for protein-protein interaction.[1,4–6] The choice of the conical representation is motivated by the fact that the angular and radial motion can be independently modified. Patch size (hence surface coverage of patches) turns out to be an important parameter missing in spherical site models. Of course, both models are equal for sufficiently narrow patches. This distinction is to a large extent subsumed in Wertheim's TPT by a strength parameter in the Mayer *f*-function.

Since the work of Sear,[1] involving Wertheim's TPT, and its application to protein phase diagram, there has been significant activity. Recently, Gögelein *et al.*[9] provided a historical summary of models for patchy proteins and took the route of a thermodynamic high temperature perturbation theory to accommodate the Yukawa interactions between the sticky spots exterior to the hard sphere (HS) surface. More along the lines of Wertheim's theory, Bianchi *et al.*[7,21] recently considered the phase behavior of sticky colloids interacting by means of HS and patchy attraction. Wentzel and Gunton[8] accommodated solvent, again via a Wertheim TPT, using a HS potential and patchy interactions that include solvent effects.

In previous work, we used simulations to show that the addition of patchy interactions to a square well (SW) fluid served to "broaden" the vapor-liquid coexistence curve. This helped to better acknowledge experimental protein phase behavior curves, and we were able to remedy the underestimated width of vapor-liquid coexistence curve.[6] To investigate this problem analytically in a broader parameter space, we apply Wertheim's TPT, more specifically, the statistical

a)Electronic addresses: sk2794@columbia.edu.
b)Electronic mail: francesco.sciortino@phys.uniroma1.it.
c)Electronic mail: glenn.evans@oregonstate.edu.

associating fluid theory for potentials of variable range (SAFT-VR).[29] Two variations in patchy models are studied here: one a HS fluid with conical patchy interactions and the other an isotropic SW fluid with patchy interactions. One of the recent applications of SAFT-VR to such a system is due to Docherty and Galindo,[30] yet only one patchy site was considered. In contrast to the spherical site model, our results show that both the number of patches and the patchy surface coverage, rather than the number of single bond patches alone, are needed to locate the critical point. We further show that patchy HS fluids with the same number of single-bonded patches obey a law of corresponding states. There is no such a law for patchy SW fluids. Rather, they show a crossover from the behavior characteristic of fluids with isotropic short-ranged attractions to that of the patchy HS fluids when the strength of patchy interactions increases.

II. PATCHY MODEL

Our model system consists of spherical particles with circular patches arranged on the particle surface. No patches overlap. Particles interact with each other through a combination of an isotropic attraction and strong anisotropic patch-patch interactions. Both interactions are described by SW potentials. The isotropic part is

$$u_i(r) = \begin{cases} \infty, & r < \sigma \\ -\varepsilon_i\varepsilon, & \sigma \le r < \lambda_i\sigma \\ 0, & r \ge \lambda_i\sigma, \end{cases} \tag{1}$$

where $\varepsilon_i\varepsilon$ is the well depth, σ is the particle diameter, λ_i controls the attraction range, and r is the distance between the centers of mass of the particles. For the patchy part, the potential has both a radial and an angular dependence. Following Kern and Frenkel,[4] we define the interpatch interaction as a product of a SW potential and an angular modulation

$$u_p(r,\Omega_i,\Omega_j) = u^{\mathrm{SW}}(r) \times f(\Omega_i,\Omega_j). \tag{2}$$

The SW part is defined analogous to Eq. (1) but with a different well width λ_p and well depth $\varepsilon_p\varepsilon$. The angular part is defined following:

$$f(\Omega_i,\Omega_j) = \begin{cases} 1 & \theta_i < \delta \quad \text{and} \quad \theta_j < \delta \\ 0 & \text{otherwise}. \end{cases} \tag{3}$$

Here θ_i is the angle between the line joining the centers of particles and the line connecting the center of particle i to the center of a patch on its surface. δ is the maximum bond-forming angle, which essentially determines the size of patches. The size of patches is further defined in terms of the surface patch coverage,

$$\chi = M \sin^2(\delta/2). \tag{4}$$

Model parameters include M (the number of patches), χ, λ_p, ε_p, λ_i, and ε_i, and can be varied as long as the values satisfy the single bond per patch condition, consistent with two of Wertheim's assumptions: No patch can be engaged in more than one bond and no pair of particles can be double bonded. It has been suggested that for a meaningful comparison between theory and simulation care must be taken to ensure the satisfaction of these assumptions.[30] When we turn on all interactions, we obtain the patchy SW fluid. When we turn off the isotropic SW attraction, the model is reduced to the patchy HS fluid.

III. HELMHOLTZ ENERGY

For the patchy fluid, the SAFT Helmholtz energy is a sum

$$A = A_{\mathrm{id}} + A_{\mathrm{sw}} + A_p \tag{5}$$

of the ideal (id), the isotropic SW (sw), and the patchy (p) interactions. The ideal part is

$$\frac{\beta A_{\mathrm{id}}}{N} = \ln(\rho\nu_T/e), \tag{6}$$

with ν_T the thermal de Broglie volume, N the number of particles, $\rho = N/V$ the number density, V the volume of system, e the base of the natural log, and β the inverse temperature. Throughout the manuscript, all quantities are reduced by the corresponding energy scale or length scale. For instance, $T^* = k_BT/\varepsilon$, $U^* = U/\varepsilon$, $C_V^* = C_V/k_B$, and $\rho^* = \rho\sigma^3$. For simplicity, the asterisk is omitted from here on.

A. Square well contribution

The Barker and Henderson[31] perturbation theory for hard-core system expresses the Helmholtz energy as a series expansion in the inverse temperature β,

$$\frac{\beta A_{\mathrm{sw}}}{N} = \frac{\beta A_{\mathrm{hs}}}{N} + \beta A_1^{\mathrm{sw}} + \beta^2 A_2^{\mathrm{sw}}, \tag{7}$$

where A_1^{sw} and A_2^{sw} are the first two perturbation terms. The HS term is obtained from the Carnahan–Starling[32] expression,

$$\frac{\beta A_{\mathrm{hs}}}{N} = \frac{4\phi - 3\phi^2}{(1-\phi)^2}, \tag{8}$$

where ϕ is the volume fraction, $\pi/6\rho$. For $1.1 \le \lambda_i \le 1.8$ the first perturbation term is[29]

$$A_1^{\mathrm{sw}} = -4\phi\varepsilon_i(\lambda_i^3 - 1)g_{\mathrm{hs}}(\sigma;\phi_{\mathrm{eff}}), \tag{9}$$

$$g_{\mathrm{hs}}(\sigma;\phi_{\mathrm{eff}}) = \frac{1 - \frac{1}{2}\phi_{\mathrm{eff}}}{(1-\phi_{\mathrm{eff}})^3}, \tag{10}$$

$$\phi_{\mathrm{eff}} = c_1\phi + c_2\phi^2 + c_3\phi^3, \tag{11}$$

where c's are given by the matrix

$$\begin{pmatrix} c_1 \\ c_2 \\ c_3 \end{pmatrix} = \begin{pmatrix} 2.258\,55 & -1.503\,49 & 0.249\,434 \\ -0.669\,27 & 1.400\,49 & -0.827\,739 \\ 10.1576 & -15.0427 & 5.308\,27 \end{pmatrix} \begin{pmatrix} 1 \\ \lambda_i \\ \lambda_i^2 \end{pmatrix}. \tag{12}$$

The fluctuation term A_2^{sw} is given directly by the first density

derivative of A_1^{sw} using the local compressibility approximation,[33]

$$A_2^{sw} = \frac{1}{2}\varepsilon_i \kappa_{hs} \phi \frac{\partial A_1^{sw}}{\partial \phi}, \tag{13}$$

where κ_{hs} is the HS isothermal compressibility,

$$\kappa_{hs} = \frac{(1-\phi)^4}{1+4\phi+4\phi^2}. \tag{14}$$

B. Patchy contribution

From Wertheim's TPT,[25,34] the patch-patch interaction contributes A_p to the Helmholtz energy

$$\frac{\beta A_p}{N} = \sum_{A\in\Gamma}\left(\ln X_A - \frac{X_A}{2}\right) + \frac{M}{2}, \tag{15}$$

where X_A is the fraction of molecules not bonded at site A and M is the number of the bonding sites. Equation (15) sums over all sites A in the set Γ (M in all). Wertheim's theory assumes that each patch acts as an independent interacting unit. In addition, the theory does not account for the contribution of closed loop of bonds. X_A can be solved by the mass action equation

$$X_A = \frac{1}{1+\Sigma_{B\in\Gamma}\rho X_B \Delta_{AB}}. \tag{16}$$

For our present model, the expression for $X_A = X$ can be simplified since the patchy sites are indistinguishable and only AA bonds are allowed,[20]

$$\frac{\beta A_p}{N} = M\left(\ln X - \frac{X}{2}\right) + \frac{M}{2}, \tag{17}$$

with

$$X = \frac{1}{1+M\rho X\Delta}. \tag{18}$$

It follows that X is

$$X = \frac{-1+\sqrt{1+4M\rho\Delta}}{2M\rho\Delta} = \frac{2}{1+\sqrt{1+4M\rho\Delta}}. \tag{19}$$

The patchy interaction strength Δ is defined by

$$\Delta = 4\pi\int_{\sigma}^{\lambda_p\sigma} g_{sw}(r_{12})\langle f(12)\rangle_{\omega_1,\omega_2} r_{12}^2 dr_{12}, \tag{20}$$

where $g_{sw}(r)$ is the reference fluid (SW fluid) pair correlation function, the Mayer f function $f(12) = e^{-\beta u_p(r_{12})} - 1$, and $\langle f(12)\rangle_{\omega_1,\omega_2}$ is an angle average over all orientations. For our conical site potential

$$\langle f(12)\rangle_{\omega_1,\omega_2} = (e^{\beta\varepsilon_p} - 1)\left(\frac{\chi}{M}\right)^2 \tag{21}$$

is constant over the interval $r_{12}\in[\sigma,\lambda_p\sigma]$. For the short-ranged patchy interaction, $g_{sw}(r_{12})r_{12}^2$ is assumed to be constant over $\sigma \le r \le \lambda_p\sigma$.[35] Since TPT is extremely sensitive to the pair distribution function of the reference fluid,[36] we use a realistic description of $g_{sw}(\sigma)$,[29] rather than the HS approximation

$$g_{sw}(\sigma) = g_{hs}(\sigma) + \frac{1}{4}\left(\frac{\partial \beta A_1^{sw}}{\partial \phi} - \frac{\lambda}{3\phi}\frac{\partial \beta A_1^{sw}}{\partial \lambda}\right). \tag{22}$$

$g_{hs}(\sigma)$ can be approximated by the Carnahan–Starling[32] equation,

$$g_{hs}(\sigma) = \frac{1-1/2\phi}{(1-\phi)^3}. \tag{23}$$

Therefore,

$$\Delta = 4\pi\sigma^3 g_{sw}(\sigma)(e^{\beta\varepsilon_p} - 1)\left(\frac{\chi}{M}\right)^2(\lambda_p - 1). \tag{24}$$

Δ has a density dependence only in $g_{sw}(\sigma)$ and the temperature dependence explicitly in $\beta\varepsilon_p$. From the above expressions, we see that the Helmholtz energy is independent of the arrangement geometry of patches.

Combining the contributions from the ideal part, the isotropic SW part and patchy part, we obtain the total Helmholtz energy of patchy fluid. Given $\beta A/N$, we find the pressure and chemical potential through

$$\frac{\beta p}{\rho} = \phi\left(\frac{\partial(\beta A/N)}{\partial\phi}\right)_T, \tag{25}$$

$$\beta\mu = \frac{\beta A}{N} + \frac{\beta p}{\rho}. \tag{26}$$

The vapor-liquid coexistence curve is determined from the Gibbs equilibrium conditions, i.e., equality of chemical potentials and pressures of coexisting phases. The spinodal is derived from $(\partial p/\partial\phi)_T = 0$ and the critical point from the conditions $(\partial p/\partial\phi)_T = (\partial^2 p/\partial\phi^2)_T = 0$.

Noro and Frenkel[37] suggested that the second virial coefficient can be used as a scaling parameter to query the corresponding states behavior for fluids with isotropic short-ranged attractions. Assuming that the patchy interaction range is always shorter ranged than that of isotropic SW interaction, the second virial coefficient of the patchy SW fluids is given by

$$\frac{B_2}{B_2^{hs}} = 1 - (\lambda_p^3 - 1)[\chi^2(e^{\beta(\varepsilon_p+\varepsilon_i)} - 1) + (1-\chi^2)(e^{\beta\varepsilon_i} - 1)] - (\lambda_i^3 - \lambda_p^3)(e^{\beta\varepsilon_i} - 1), \tag{27}$$

where B_2^{hs} is the second virial coefficient of HS fluid. The limits of B_2 for patchy HS fluids or pure SW fluids can be recovered for $\lambda_i = 1$ and $\varepsilon_i = 0$ or $\lambda_p = 1$, respectively.

Wertheim's theory for the Helmholtz energy of patchy HS fluids provides information about the mean potential energy, the heat capacity, cluster distributions, and the number of bonds per particle. One can unambiguously define the bond between two particles for the SW case. The probability

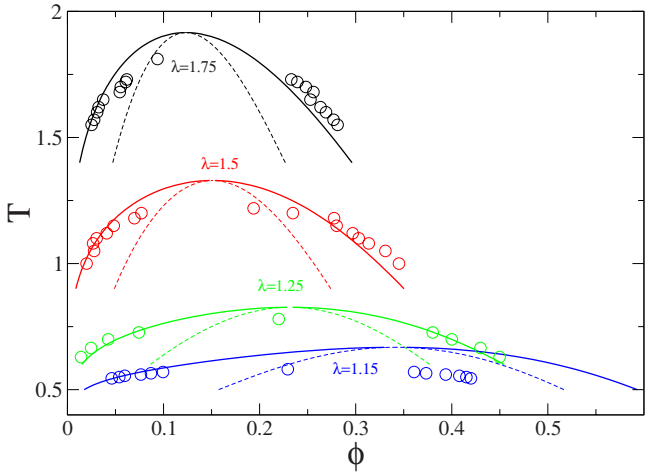

FIG. 1. (Color online) Comparison of theoretical predictions and simulation data for the vapor-liquid coexistence curves of pure SW fluids. The open circles are from MC data of Vega *et al.* (Ref. 38) and of Liu *et al.* (Ref. 39). The solid lines (binodal) and dashed lines (spinodal) are theoretical predictions.

that an arbitrary patch is bonded is given by $p_b=1-X$. So the average number of bonds per particle is equal to

$$N_B = M(1-X), \tag{28}$$

which differs the total number of bonds divided by the number of particles by a factor of 2. The configurational energy due to the patchy interaction is given by

$$\frac{U_p}{N} = \left(\frac{\partial(\beta A/N)}{\partial\beta}\right)_V, \tag{29}$$

that is,

$$\frac{U_p}{N} = M\left(\frac{1}{X}-\frac{1}{2}\right)\left(\frac{\partial X}{\partial\beta}\right)_V = -\frac{N_B}{2}\frac{\varepsilon_p}{1-e^{-\beta\varepsilon_p}}. \tag{30}$$

We note that bonding usually takes place when $e^{-\beta\varepsilon_p}\ll 1$, hence one should expect that $U_p/N=-N_B/2\varepsilon_p$, which is exactly the fraction of bonds times $-M/2\varepsilon_p$.

Likewise, the heat capacity at constant volume due to bonding can be obtained through

$$\frac{C_V^p}{N} = \left(\frac{\partial(U_p/N)}{\partial T}\right)_V, \tag{31}$$

so,

$$\frac{C_V^p}{N} = \frac{N_B}{2}\left(\frac{\beta\varepsilon_p}{1-e^{-\beta\varepsilon_p}}\right)^2\left(\frac{X}{2-X}-e^{-\beta\varepsilon_p}\right). \tag{32}$$

To account for the ideal part contribution, the C_V/N of the patchy HS fluid should be a sum of C_V^p/N and 3 (translational and rotational degrees of freedom). Based on the fact that the number of clusters present at equilibrium is decreased by 1 for every bond formed, Chapman *et al.*[35] obtained the density of clusters

$$\rho_{\text{cluster}} = \rho\left(1-\frac{1}{2}\sum_A (1-X_A)\right). \tag{33}$$

For our model with indistinguishable patches, the equation

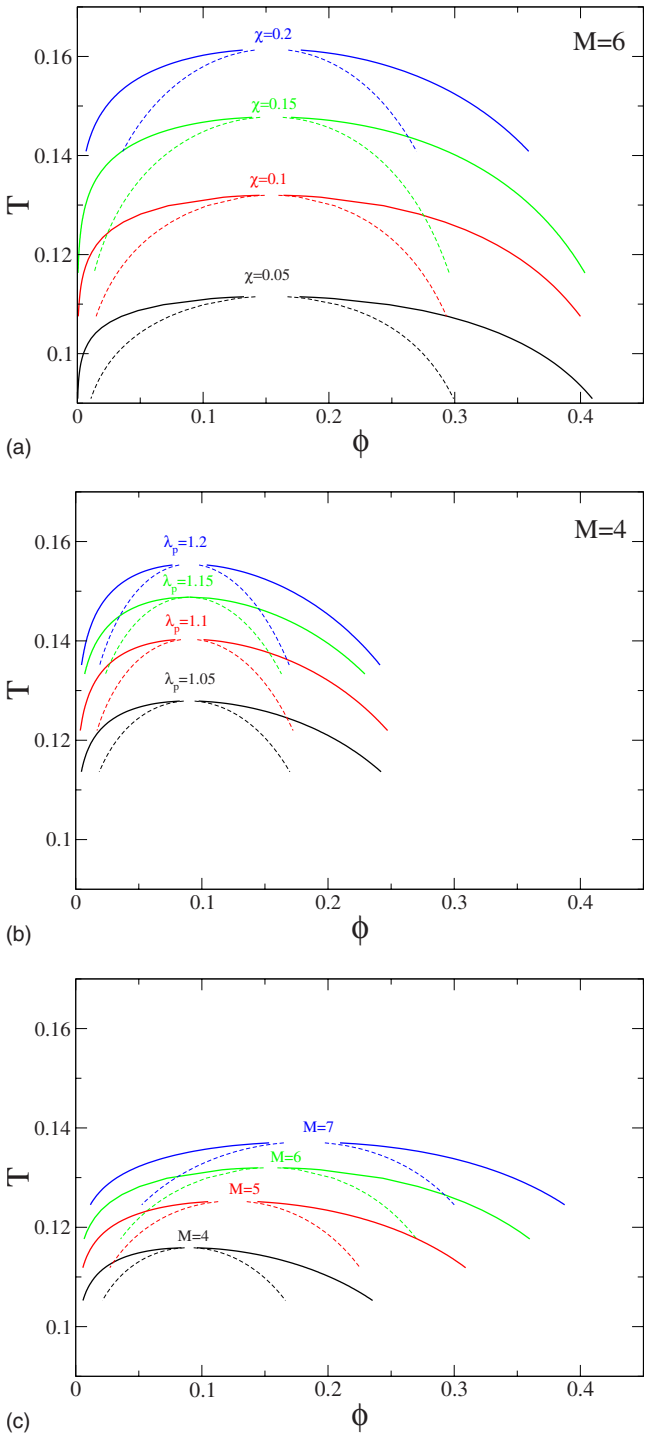

FIG. 2. (Color online) Vapor-liquid coexistence curves of patchy HS fluids from predictions of Wertheim's theory (solid lines for binodals and dashed lines for spinodals). (a) Effect of the surface coverage (χ) with $M=6$, $\lambda_p=1.05$. (b) Effect of the potential range of patchy interactions (λ_p) with $M=4$, $\chi=0.15$. (c) Effect of the number of patches (M) with $\chi=0.1$, $\lambda_p=1.05$.

becomes

$$\rho_{\text{cluster}} = \rho\left(1-\frac{M}{2}(1-X)\right), \tag{34}$$

and the average cluster size is approximated by

TABLE I. Critical properties for patchy HS fluids with $\lambda_i=1$ and $\varepsilon_i=0$.

	λ_p	χ	β_c	ϕ_c	B_2^c/B_2^{hs}	p_m^c
$M=3$	1.05	0.12	9.589	0.049 55	−32.14	0.634
	1.07	0.12	9.252	0.049 55	−32.78	0.634
	1.119	0.045	10.68	0.049 58	−34.49	0.634
	1.119	0.075	9.665	0.049 52	−34.55	0.634
	1.119	0.12	8.722	0.049 55	−34.44	0.634
	1.119	0.1575	8.177	0.049 56	−34.40	0.634
$M=4$	1.01	0.16	9.301	0.0899	−7.492	0.493
	1.05	0.1	8.63	0.09	−7.821	0.493
	1.05	0.15	7.82	0.0896	−7.827	0.492
	1.05	0.16	7.687	0.0899	−7.792	0.492
	1.07	0.16	7.353	0.090	−7.986	0.493
	1.09	0.16	7.106	0.0899	−8.201	0.493
	1.1	0.15	7.13	0.0898	−8.293	0.493
	1.119	0.12	7.398	0.0899	−8.426	0.493
	1.119	0.16	6.822	0.0899	−8.416	0.493
	1.119	0.21	6.278	0.0899	−8.407	0.493
	1.15	0.15	6.72	0.0899	−8.702	0.493
	1.2	0.15	6.44	0.0899	−9.244	0.494
$M=5$	1.01	0.2	8.205	0.1242	−3.434	0.416
	1.05	0.1	7.99	0.1245	−3.650	0.418
	1.05	0.2	6.596	0.1242	−3.610	0.416
	1.07	0.2	6.26	0.1242	−3.701	0.416
	1.09	0.2	6.01	0.1242	−3.797	0.417
	1.119	0.125	6.668	0.1242	−3.926	0.416
	1.119	0.2	5.731	0.1242	−3.931	0.417
	1.119	0.2625	5.189	0.1242	−3.928	0.418
$M=6$	1.05	0.05	8.97	0.1554	−2.098	0.370
	1.05	0.1	7.578	0.155	−2.079	0.369
	1.05	0.15	6.77	0.149	−2.087	0.360
	1.05	0.2	6.2	0.1516	−2.100	0.365

$$N_{\mathrm{cluster}} = \frac{\rho}{\rho_{\mathrm{cluster}}} = \frac{1}{1 - \frac{M}{2}(1-X)}. \tag{35}$$

From Wertheim theory we can also estimate the density of particles with M patches bonded at n patches. The density of monomers (that is, no patch is bonded)is given by

$$\rho_0 = \rho X^M. \tag{36}$$

Similarly, the density of particles with one bond is

$$\rho_1 = \rho M X^{M-1}(1-X). \tag{37}$$

Generalizing from above equations, the density of particles with n bonds is

$$\rho_n = \rho \binom{M}{n} X^{M-n}(1-X)^n, \tag{38}$$

where $\binom{M}{n}$ is the binomial coefficient of M and n. Certainly, $\Sigma_{i=0}^{M}\rho_i=\rho$.

IV. RESULTS AND DISCUSSION

A. Pure square well fluids

We first compare our perturbation scheme for the pure SW fluids with Monte Carlo (MC) simulation data, as shown in Fig. 1. The theoretical predictions are in good agreement with simulation.[38,39] Comparison has been shown by Gil-Villegas *et al.*[29] and are presented here merely for completeness.

B. Patchy hard sphere fluids

Shown in Fig. 2 are the binodals and spinodals from Wertheim's theory for different sets of parameters of patchy HS fluids. Our results are broadly consistent with previous data,[1,3,8] except that in the previous work, the authors omitted an M in the formula of X and this resulted in the underestimated critical temperatures. We also notice that the model used by Bianchi *et al.*[7,21] essentially predetermined patch size through specifying the interaction range of patchy interactions, so they found that critical properties only depend on M. Our model allows us to independently vary the patch size, the number of patches, and the interaction range of patchy interaction.

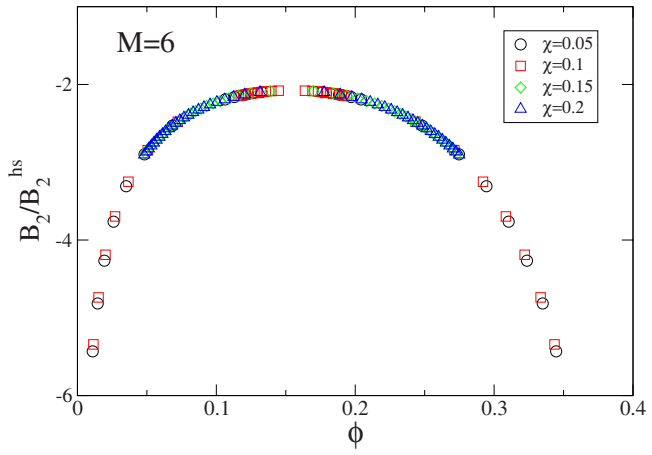

FIG. 3. (Color online) Law of the corresponding states of patchy HS fluids with $M=6$, $\lambda_p=1.05$.

First, we vary χ, essentially the patch size, for $M=6$ and $\lambda_p=1.05$. The critical temperature increases with increasing χ, while the critical density remains intact. Second, we find that with increasing λ_p, the critical temperature increases again, whereas the critical density is nearly constant. In contrast, the critical density of fluids with an isotropic attractive potential is known to increase as the interaction range decreases (see Fig. 1). The results of TPT predict that the critical density of patchy HS fluids with constant M is insensitive to the patch surface coverage and the patchy interaction range, which is inconsistent with MC results that the critical density does show χ and λ_p dependence.[40] Third, we present phase diagrams for varying M and fixed $\chi=0.1$ and $\lambda_p=1.05$. The critical temperature shifts to lower ones with decreasing M, while the critical density decreases with decreasing M. The coexistence region shrinks as we decrease M.[21]

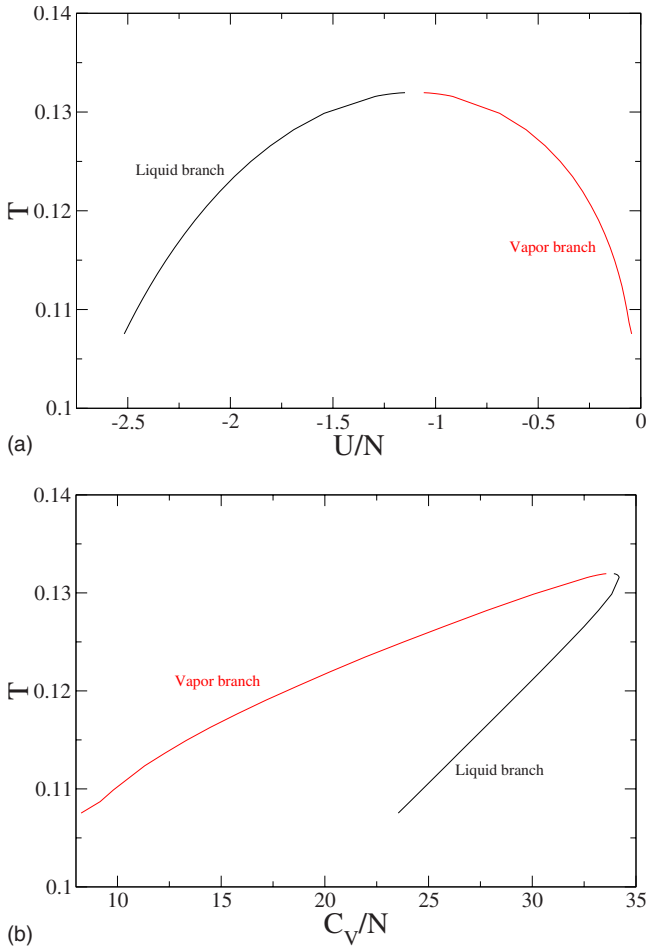

FIG. 4. (Color online) (a) Equilibrium potential energies and (b) heat capacities at constant volume for the coexisting vapor and liquid phases of patchy HS fluid with $M=6$, $\lambda_p=1.05$, and $\chi=0.1$.

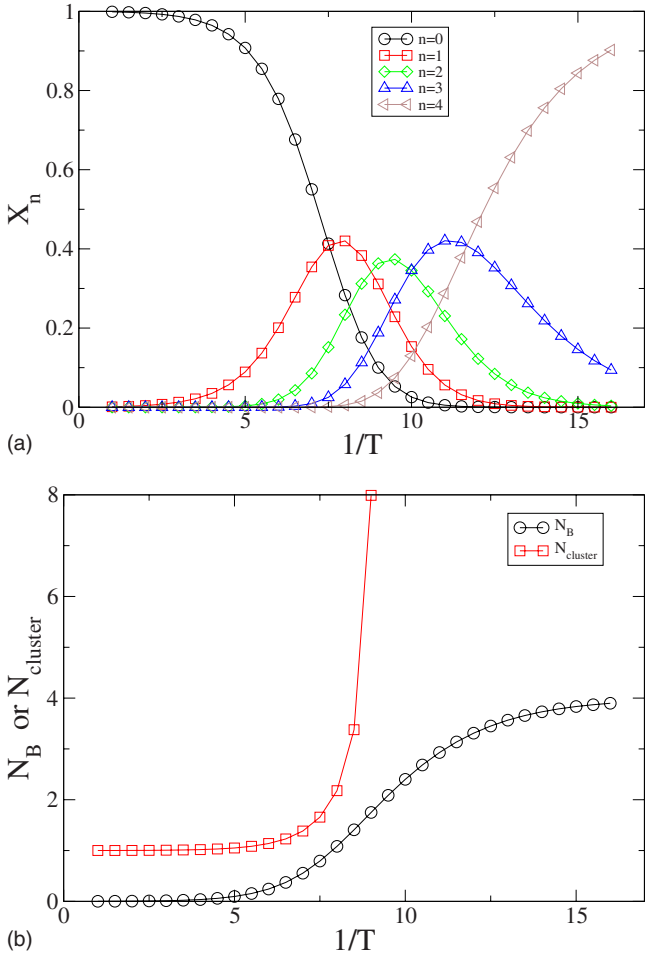

FIG. 5. (Color online) (a) Inverse temperature dependence of fractions of particles with n bonded patches and (b) the average number of bonds per particle and the average cluster size of patchy HS fluids with $M=4$, $\chi=0.1$, and $\lambda_p=1.05$.

Recently, Noro and Frenkel[37] proposed a generalized law of corresponding states (GLCS) for variable range attractive fluids using the second virial coefficient (B_2) as the scaling parameter. Foffi and Sciortino[40] extended this idea to patchy fluids provided the one bond per patch constraint is fulfilled. It is interesting to check GLCS for our theoretical data. We present B_2 values at the critical points (B_2^c) in Table I for HS patchy fluids. We can see that each M is characterized by a specific B_2^c value, that is, GLCS holds for each number of patches—$B_2^c/B_2^{\mathrm{hs}} \sim f(M)$. Although a closer look at B_2^c values shows that small variations exist, the differences in B_2^c between different M are much larger than those at the same M. Furthermore, our data show not only that the critical B_2^c's have constant values, but that the coexistence curves of each M class fall onto universal curves (see Fig. 3). Our

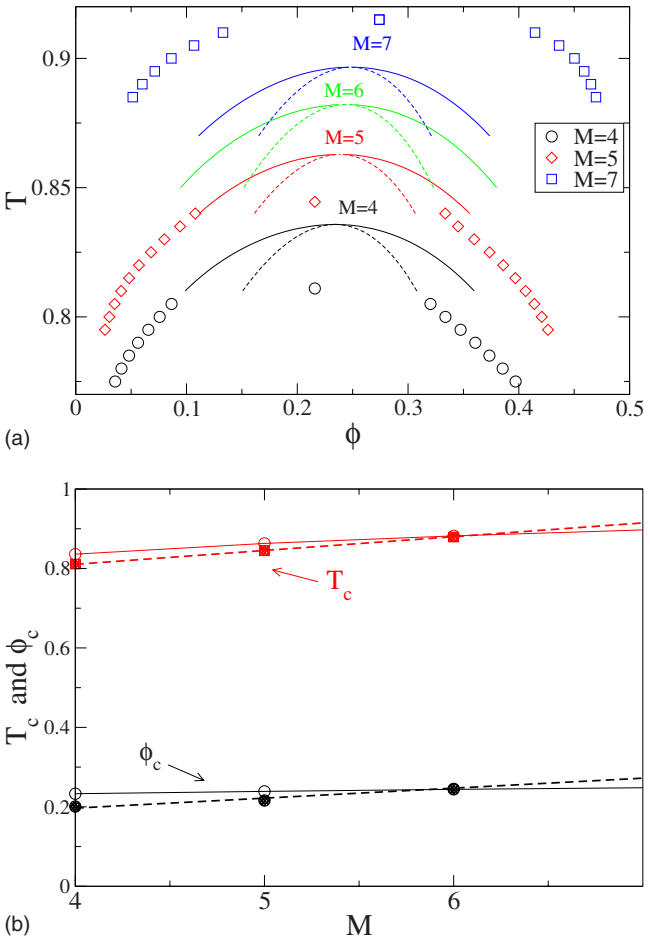

FIG. 6. (Color online) (a) Effect of the number of patches on the vapor-liquid coexistence curves and (b) the critical properties of patchy SW fluids with $\lambda_p=1.05$, $\varepsilon_p=5$, $\chi=0.1$, $\lambda_i=1.15$, and $\varepsilon_i=1$. MC simulation data (Ref. 6) are shown by symbols and theoretical binodals and spinodals are shown by lines and dash lines in panel (a). MC simulation data (Ref. 6) are shown by filled symbols and theoretical predictions by open symbols and all lines serve as guides to eyes in panel (b).

data provide the theoretical evidence that the anisotropic HS fluids with different sets of parameters obey a GLCS for the same M. We also report p_m^c defined as the potential energy at the critical point normalized by the energy of fully bonded system in Table I.

$$p_m^c = \frac{U_p^{\text{critical}}}{U_p^{\text{fully bonded}}} = \frac{1 - X^c}{1 - e^{-\beta_c \varepsilon_p}}. \tag{39}$$

A constant p_m^c is observed for each M, which confirms the existence of a GLCS for each M and suggests that p_m^c might be the better scaling parameter.[40]

By means of TPT, we calculate the potential energy and heat capacity for coexisting phases, as shown in Fig. 4. The fraction of particles with varying number of attached bonds is presented in Fig. 5(a). We also show the average number of bonds per particle and the average cluster size N_{cluster} in Fig. 5(b). According to Eq. (35), the average cluster size diverges when $X=1-2/M$, and as seen in Fig. 5(b), this divergence occurs as β approaches 9.3.

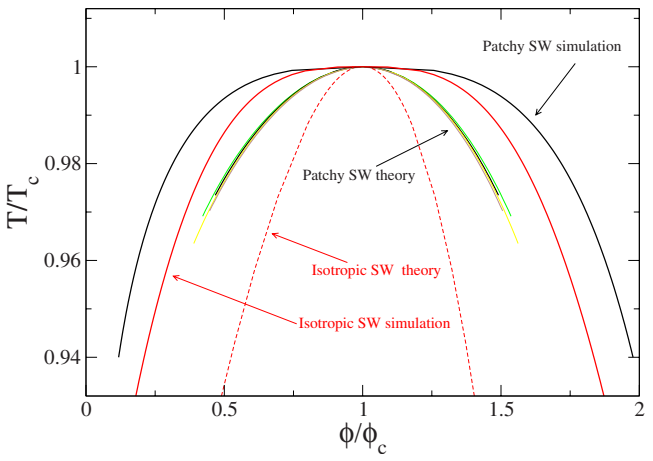

FIG. 7. (Color online) Comparison of Wertheim's theory calculations (dashed lines) and simulations (Refs. 6 and 39) (solid lines) in reduced temperature and reduced density plane. Model parameters are the same as those in Fig. 6. Note that the width of binodals of patchy SW fluids is much broader than that of isotropic fluids in both cases.

C. Patchy square well fluids

Next, consider the patchy SW model with a SW fluid as the reference fluid. We compare the TPT predictions and MC calculations[6] of the binodals in Fig. 6(a), the critical parameters in Fig. 6(b) and in the reduced temperature and reduced density plane in Fig. 7. Theory overestimates the critical temperatures for the $M=4$ and $M=5$ models, whereas it underestimates those of the $M=7$ model. The source of the discrepancies are myriad: Wertheim theory is accurate in the low bonding regime, it ignores the directionality of the bonding interactions (no steric blocking allowed, no geometric considerations), and it is perturbative.[4,41] However, given the complexity of the fluid, Wertheim's TPT gives at least qualitative agreement with simulation, and more importantly, it gives the right M dependence of critical parameters. Wertheim's theory confirms that there exists a universal coexistence curve for patchy SW fluids with the same set of model parameters used in our previous MC simulations[6] that is much broader than those of SW fluids if we use the critical

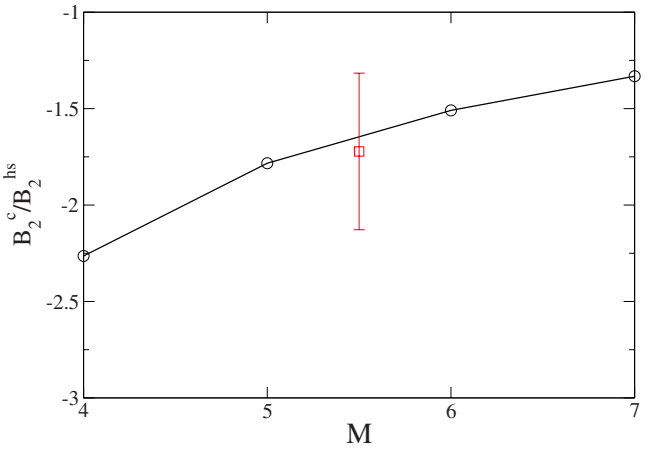

FIG. 8. (Color online) Critical second virial coefficients for patchy SW fluids. Circles are data points. The mean is shown by a square and the standard deviation is shown by the bar. Patchy SW fluids share the same set of parameters as those in Fig. 6.

TABLE II. Critical properties for patchy SW fluids where $\varepsilon_i=1$.

	λ_p	ε_p	χ	λ_i	T_c	ϕ_c	B_2^c/B_2^{hs}	$(B_2^c)^{iso}/B_2^{hs}$	$(B_2^c)^p/B_2^{hs}$
$M=4$	1.03	5	0.1	1.15	0.8038	0.2529	−1.901	−0.2864	−0.4654
	1.05	5	0.1	1.15	0.8358	0.2342	−2.264	−0.2024	−0.6232
	1.1	5	0.1	1.15	0.8878	0.2209	−2.926	−0.0857	−0.9208
	1.15	5	0.1	1.15	0.9247	0.192	−3.425	−0.0151	−1.156
$M=5$	1.05	5	0.05	1.15	0.7711	0.2773	−1.327	−0.3843	−0.2576
	1.05	5	0.1	1.15	0.8629	0.2386	−1.783	−0.1388	−0.5162
	1.05	5	0.15	1.15	0.9382	0.2273	−2.105	0.0086	−0.7281
	1.05	5	0.2	1.15	1.008	0.2021	−2.292	0.1162	−0.8930
	1.05	1	0.15	1.15	0.6738	0.3395	−0.8301	−0.7767	−0.0121
	1.05	3	0.15	1.15	0.7474	0.2878	−1.199	−0.4643	−0.1928
	1.05	5	0.15	1.15	0.9382	0.2273	−2.105	0.0086	−0.7281
	1.05	7	0.15	1.15	1.183	0.1719	−2.751	0.3079	−1.313
$M=6$	1.05	5	0.1	1.1	0.8306	0.2284	−1.929	0.2277	−0.6470
	1.05	5	0.1	1.15	0.8822	0.2433	−1.509	−0.0973	−0.4545
	1.05	5	0.1	1.2	0.9378	0.2435	−1.329	−0.3866	−0.3243
	1.05	5	0.1	1.25	0.996	0.234	−1.295	−0.6482	−0.2371
$M=7$	1.05	5	0.1	1.15	0.8967	0.2482	−1.332	−0.0679	−0.4146

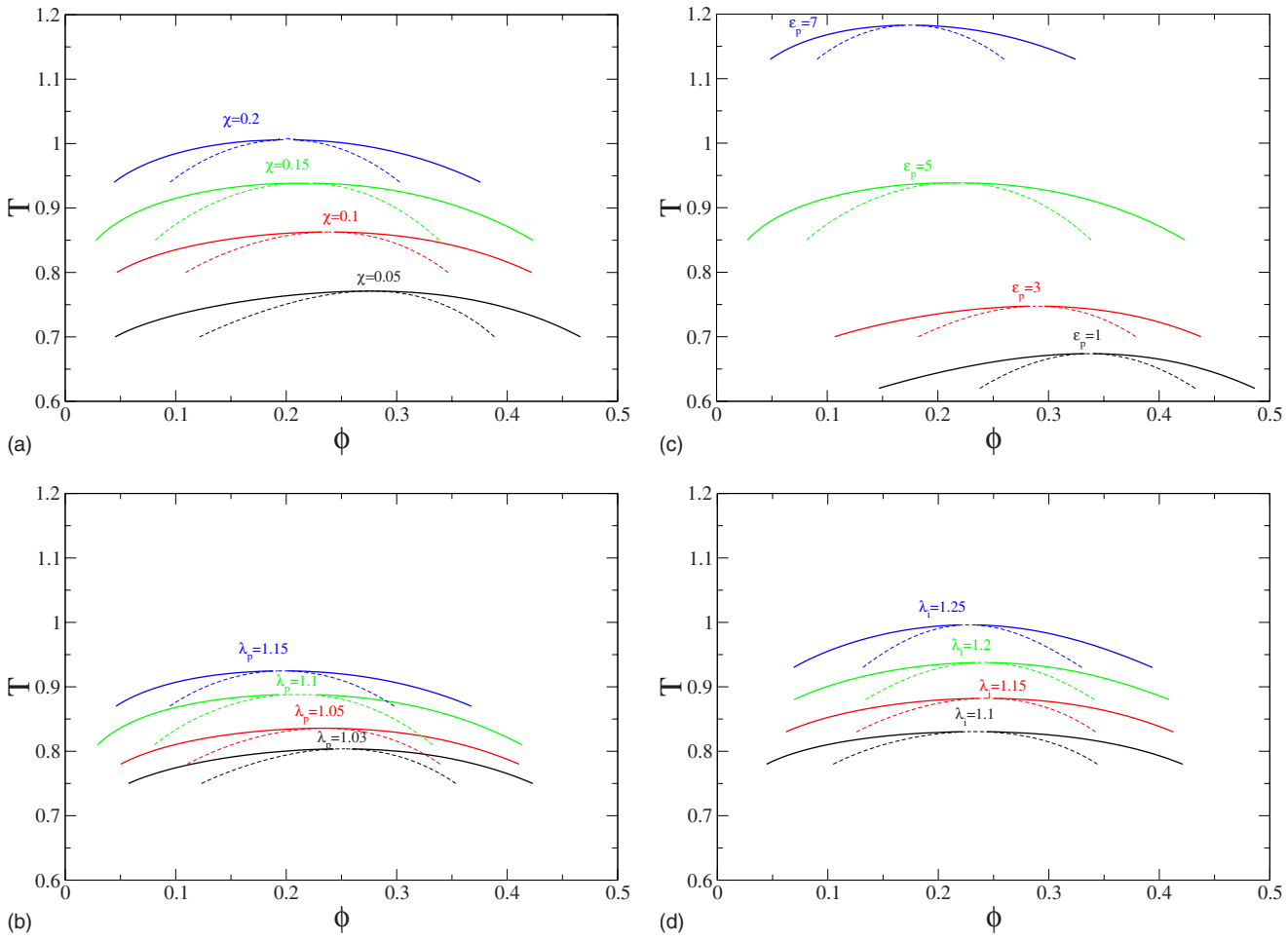

FIG. 9. (Color online) Vapor-liquid coexistence curves of patchy SW fluids from predictions of Wertheim's theory (solid lines for binodals and dashed lines for spinodals). (a) Effect of the surface coverage of patches with $\lambda_p=1.05$, $\varepsilon_p=5$, $M=5$, $\lambda_i=1.15$, and $\varepsilon_i=1$. (b) Effect of the potential range of patchy interactions with $\varepsilon_p=5$, $M=4$, $\chi=0.1$, $\lambda_i=1.15$, and $\varepsilon_i=1$. (c) Effect of the strength of patchy interactions with $\lambda_p=1.05$, $\chi=0.15$, $M=5$, $\lambda_i=1.15$, and $\varepsilon_i=1$. (d) Effect of the potential range of isotropic SW interactions with $\lambda_p=1.05$, $\varepsilon_p=5$, $\chi=0.1$, $M=6$, and $\varepsilon_i=1$.

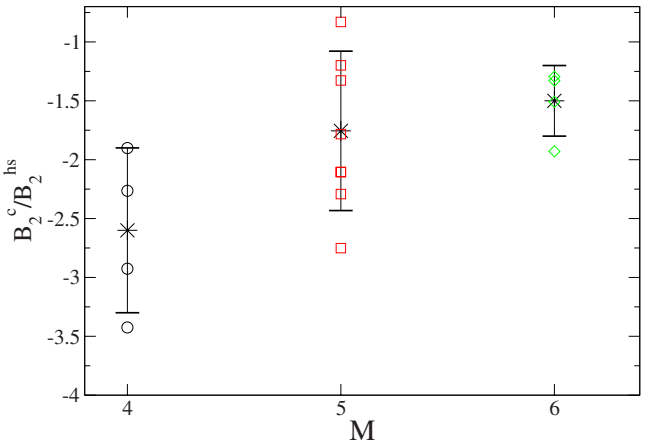

FIG. 10. (Color online) Critical second virial coefficients of patchy SW fluids with different sets of parameters studied in Fig. 9. The analytical data are shown by open symbols. The means and standard deviations for each M are shown by asterisks and bars.

properties as the scaling parameters (see Fig. 7). We further check B_2 as the scaling variable in Fig. 8 and Table II. The data show that B_2^c/B_2^{hs} is not constant for fixed M, much less for the whole coexistence curves. We also note that the critical density displays less sensitivity to M as compared with that of the patchy HS fluids.

We explore patchy SW fluids in the broader parameter space and vary χ, λ_p, ε_p, and λ_i shown in Fig. 9. With increasing χ, λ_p, ε_p, and λ_i, the critical temperature increases, reflecting stronger association. The critical density decreases with increasing χ, λ_p, and ε_p, while the critical density shows a nonmonotonic trend that first increases then decreases with increasing λ_i. The second virial coefficient B_2 at critical points for patchy SW fluids (see Table II and Fig. 10), when reduced by B_2^{hs}, is scattered for each M class for all patchy SW fluids. A law of corresponding states is not observed. We also tried the critical properties as scaling variables, and no master curve is observed. It is not unexpected since the patchy SW fluid can be reduced to the two extreme cases, each governed by a different energy scale. One is the spherical short-ranged attractive fluid that should behave in the same way, irrespective of the specific potential form and interaction range; the other is the patchy HS fluid that behave similarly only if the number of patches is the same and the single-bonded condition is satisfied. Through the competition of these two components, we would expect that the patchy SW fluid should show the crossover from the class dominated by the isotropic short-ranged attraction to the class completely controlled by the patchy HS potential. It is clearly shown for the $M=5$ case in Table II that as ε_p increases, the increasing $(B_2^c)^{iso}$ denotes the weaker contribution of the isotropic part to the total B_2, while the decreasing $(B_2^c)^p$ demonstrates the stronger contribution of patchy part to the total B_2. The patchy SW fluid with $M=5$ shifts to the patchy HS behavior, when the relative weight of patchy interaction increases and essentially recovers the patchy HS value of B_2^* when $\varepsilon_p=7$.

V. CONCLUSION

Wertheim's TPT has been applied to a study of the vapor-liquid equilibrium of fluids with strong patchy interaction regions. The agreement between the theory and the MC simulation suggests that Wertheim's theory is a promising tool for capturing the broad outlines of phase behavior. We provide theoretical evidence that different patchy HS fluids with the same number of single-bonded patches obey a GLCS. Furthermore, we have demonstrated that the patchy SW fluid illustrates a crossover from the behavior of the isotropic short-ranged attractive fluid to that of the patchy HS fluid.

ACKNOWLEDGMENTS

The authors thank the National Science Foundation (ITR Grant Nos. DMR-0313101 and CHE-0314549) and the Department of Energy for funding this research.

[1] R. P. Sear, J. Chem. Phys. **111**, 4800 (1999).
[2] A. Lomakin, N. Asherie, and G. B. Benedek, Proc. Natl. Acad. Sci. U.S.A. **96**, 9465 (1999).
[3] N. M. Dixit and C. F. Zukoski, J. Chem. Phys. **117**, 8540 (2002).
[4] N. Kern and D. Frenkel, J. Chem. Phys. **118**, 9882 (2003).
[5] J. Chang, A. M. Lenhoff, and S. I. Sandler, J. Chem. Phys. **120**, 3003 (2004).
[6] H. Liu, S. K. Kumar, and F. Sciortino, J. Chem. Phys. **127**, 084902 (2007).
[7] E. Bianchi, P. Tartaglia, E. Zaccarelli, and F. Sciortino, J. Chem. Phys. **128**, 144504 (2008).
[8] N. Wentzel and J. D. Gunton, J. Phys. Chem. B **112**, 7803 (2008).
[9] C. Gögelein, G. Nägele, R. Tuinier, T. Gibaud, A. Stradner, and P. Schurtenberger, J. Chem. Phys. **129**, 085102 (2008).
[10] J. Kolafa and I. Nezbeda, Mol. Phys. **61**, 161 (1987).
[11] C. Vega and P. A. Monson, J. Chem. Phys. **109**, 9938 (1998).
[12] T. B. Peery and G. T. Evans, J. Chem. Phys. **118**, 2286 (2003).
[13] C. De Michele, S. Gabrielli, P. Tartaglia, and F. Sciortino, J. Phys. Chem. B **110**, 8064 (2006).
[14] F. Romano, P. Tartaglia, and F. Sciortino, J. Phys.: Condens. Matter **19**, 322101 (2007).
[15] D. Ghonasgi and W. Chapman, Mol. Phys. **79**, 291 (1993).
[16] E. Vakarin, Y. Duda, and M. F. Holovko, J. Stat. Phys. **88**, 1333 (1996).
[17] E. Vakarin, Y. Duda, and M. F. Holovko, Mol. Phys. **90**, 611 (1997).
[18] Y. Duda, J. Chem. Phys. **109**, 9015 (1998).
[19] Y. Duda, C. J. Segura, E. Vakarin, M. F. Holovko, and W. G. Chapman, J. Chem. Phys. **108**, 9168 (1998).
[20] S. H. Huang and M. Radosz, Ind. Eng. Chem. Res. **29**, 2284 (1990).
[21] E. Bianchi, J. Largo, P. Tartaglia, E. Zaccarelli, and F. Sciortino, Phys. Rev. Lett. **97**, 168301 (2006).
[22] V. N. Manoharan, M. T. Elsesser, and D. J. Pine, Science **301**, 483 (2003).
[23] Y.-S. Cho, G.-R. Yi, J.-M. Lim, S.-H. Kim, V. N. Manoharan, D. J. Pine, and S.-M. Yang, J. Am. Chem. Soc. **127**, 15968 (2005).
[24] Z. Zhang, A. S. Keys, T. Chen, and S. C. Glotzer, Langmuir **21**, 11547 (2005).
[25] M. S. Wertheim, J. Stat. Phys. **35**, 19 (1984).
[26] M. S. Wertheim, J. Stat. Phys. **35**, 34 (1984).
[27] M. S. Wertheim, J. Stat. Phys. **42**, 459 (1986).
[28] F. Sciortino, E. Bianchi, J. F. Douglas, and P. Tartaglia, J. Chem. Phys. **126**, 194903 (2007).
[29] A. Gil-Villegas, A. Galindo, P. J. Whitehead, S. J. Mills, G. Jackson, and A. N. Burgess, J. Chem. Phys. **106**, 4168 (1997).
[30] H. Docherty and A. Galindo, Mol. Phys. **104**, 3551 (2006).
[31] J. A. Barker and D. Henderson, J. Chem. Phys. **47**, 2856 (1967).
[32] N. F. Carnahan and K. E. Starling, J. Chem. Phys. **51**, 635 (1969).
[33] J. A. Barker and D. Henderson, Rev. Mod. Phys. **48**, 587 (1976).
[34] G. Jackson, W. G. Chapman, and K. E. Gubbins, Mol. Phys. **65**, 1 (1988).
[35] W. G. Chapman, G. Jackson, and K. E. Gubbins, Mol. Phys. **65**, 1057 (1988).
[36] E. A. Muller, K. E. Gubbins, D. M. Tsangaris, and J. J. de Pablo,

J. Chem. Phys. **103**, 3868 (1995).
[37] M. G. Noro and D. Frenkel, J. Chem. Phys. **113**, 2941 (2000).
[38] L. Vega, E. de Miguel, L. F. Rull, G. Jackson, and I. A. McLure, J. Chem. Phys. **96**, 2296 (1992).
[39] H. Liu, S. Garde, and S. Kumar, J. Chem. Phys. **123**, 174505 (2005).
[40] G. Foffi and F. Sciortino, J. Phys. Chem. B **111**, 9702 (2007).
[41] R. A. Curtis, H. W. Blanch, and J. M. Prausnitz, J. Phys. Chem. B **105**, 2445 (2001).